File S1

Supporting Text: Evaluation of the *Poisson* assumption of the analytical model

We modeled the distribution of TE copy number as *Poisson,* which has been well established in the literature. However, this approximation holds true mainly when the TE population is at near equilibrium and the TE copy number is large. The key part of our model is the spread of a newly invaded TE family, during which the TE population is not at equilibrium and the copy number may be low. To investigate how the deviation from *Poisson* approximation may influence the predictions of our analytical models, we performed full Monte Carlo simulations to evaluate the potential impacts of this assumption.

Monte Carlo Simulations

We used the following Monte Carlo simulation to address this issue. The host population size is 100,000. Each host individual genome is comprised of two parental complements of three chromosomes, each of which has 1,000 potential TE insertion sites and a host locus. Crossover is modeled as *Poisson* process and the crossover rate is set as 0.001 between two potential TE insertion sites, making it averagely one crossover per chromosome per generation. At generation zero, the 0.1% of the population contain on average μ_0 copies of the TE (distribution is *Poisson*). Independently chosen 0.1% of the population have the beneficial allele at the host locus.

A new member of the next generation is simulated through the following steps. Two parents are first chosen and each parent contributes a haploid genome to the offspring (assuming independent assortment and crossing over as described above). Neither TE insertions nor the host locus influence the transmission. Each TE insertion of the offspring then independently undergoes a single replicative transposition with probability equal to the transposition rate *u*, which changes according to the cytotype of the parent (u_0 in hybrid dysgenic cross and u_1 in the other crosses) and the host locus genotype of the offspring (*u(1-d)* in homozygotes of beneficial allele, *u(1-hd)* in heterozygotes of beneficial allele and *u* for the other genotype). If the total number of transposition events in an offspring is above the hybrid dysgenic threshold (*HD*), the offspring's fitness is set to zero and the offspring is not passed to the next generation. If the total number of transposition events in an offspring is below the threshold, its fitness is calculated according to the following equation ($w(n) = e^{-an-bn^2/2}$, where *n* is the total TE copy number and *a* and *b* are 10^{-5} and 10^{-6} respectively). The offspring is transmitted to the next generation with probability equal to it fitness. This process is repeated until 100,000 offspring are generated.

According to the analyses of the analytical modeling, following parameters did not have significant impacts on the dynamics of *I* and were chosen as follows for the simulation: $d = 0.5$, $h = 0.5$, $u_1 = 10^{-4}$ and $\mu_0 = 10$. As discussed in the main text, the spread of newly invaded TE family has almost no impacts on the host gene for cases where u_0 equals 0.1, which is of course less interesting case for our analysis. We thus chose $u_0 = 1$ for our simulation. We did pilot simulations with n_{HD} equals 3, 5, 7, and 10 and found no apparent differences (data not shown) and thus only the case with the greater numbers of simulations, $n_{HD} = 5$, are presented below.

Results of Simulations

Following figures showed the averaged result of 1,000 Monte Carlo simulations for proportion of *P cytotype* (Figure S1), TE copy number (Figure S2) and the frequency of host beneficial allele (Figure S3 and Figure S4), comparing with the prediction of analytical model. The most critical part of our analytical model is from the invasion of the newly invaded TE family to its reaching equilibrium in the population, which takes approximately 100 generations after its first invasion.

Simulations showed the spread and the increase in copy number of the newly invaded TE family is slower than the analytical prediction (Figure S1 and S2). The allele frequency predicted by the analytical model based on the assumed *Poisson* distribution of copy number tends to initially exceed then fall below the simulated host allele frequency (Figure S3). However, the error between analytical approximation and the simulation is always within 2% (Figure S4). Thus, our overall conclusion that the spread of a newly invaded TE family is unlikely to drive the fast evolution of interacting host genes is not sensitive to the naïve assumptions of the analytic model.

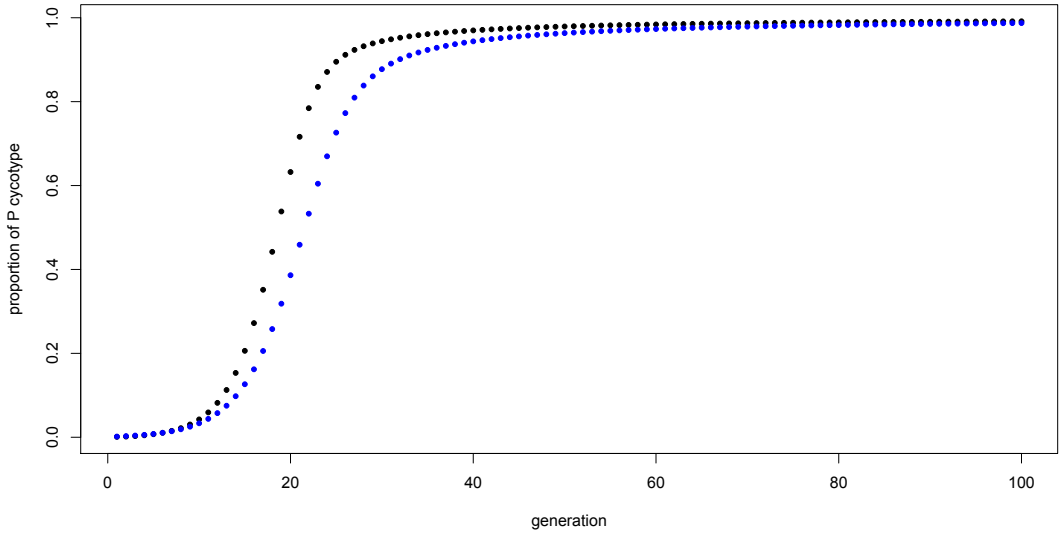

Figure S1 The proportion of *P cytotype* individuals over time. Black and blue dots are the analytical prediction and simulation results respectively.

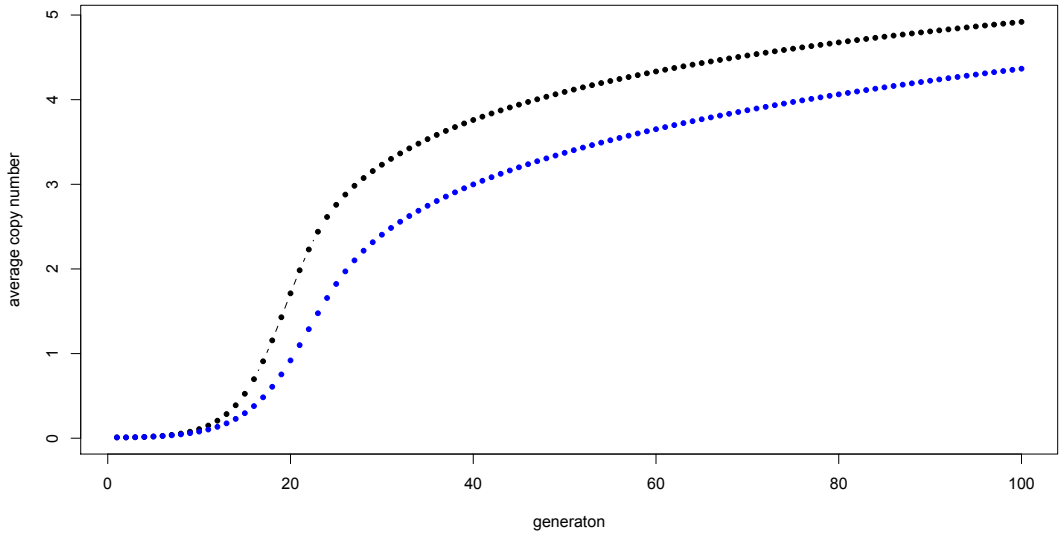

Figure S2 The averaged TE copy number over time. Black and blue dots are the analytical prediction and simulation results respectively.

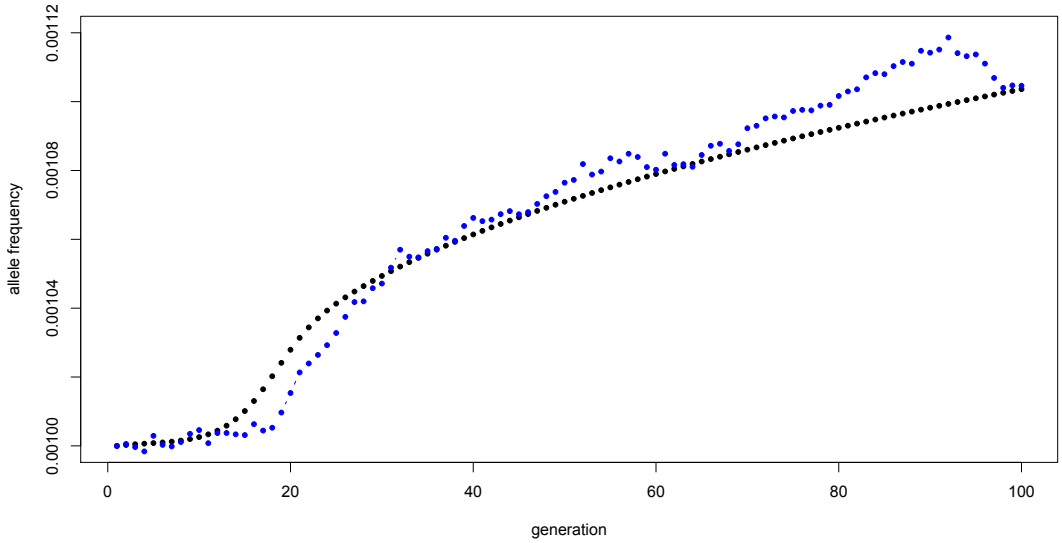

Figure S3 The frequency of host beneficial allele over time. Black and blue dots are the analytical prediction and simulation results respectively.

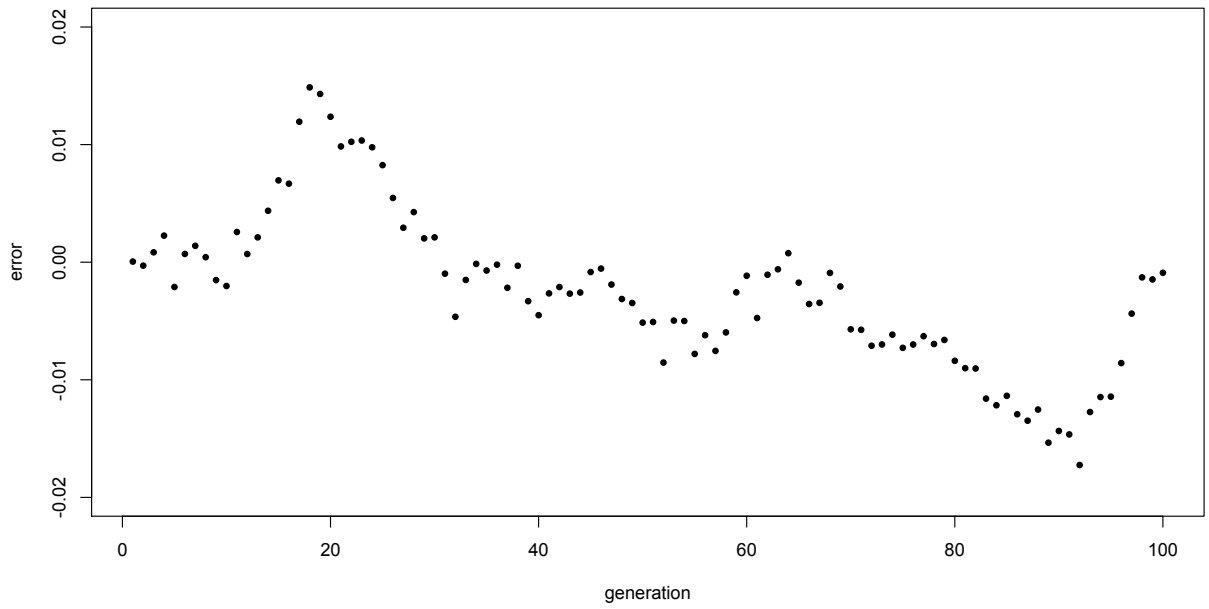

Figure S4 The errors of analytical prediction of the host beneficial allele with respect to simulations.

During the initial invasion phase, the *Poisson* distribution predicts a distribution that has larger mode than the actual simulation (Figure S5A, B). Soon after *the P cytotype* individuals in the population become common (≈ generation 35), the TE copy number distribution is nearly *Poisson* (Figure S5C, D). In addition to the fact that the *Poisson* distribution is a good approximation to the Binomial sampling when the TE copy number is large, the linkage among TE insertions also contributes to the differences between the predictions of analytical model and simulations. In simulations where there is free recombination among TE insertions, the distribution of TE copy number quickly reaches *Poisson* within 15 generations, when the *P cytotype* in the population is still rare (results not shown).

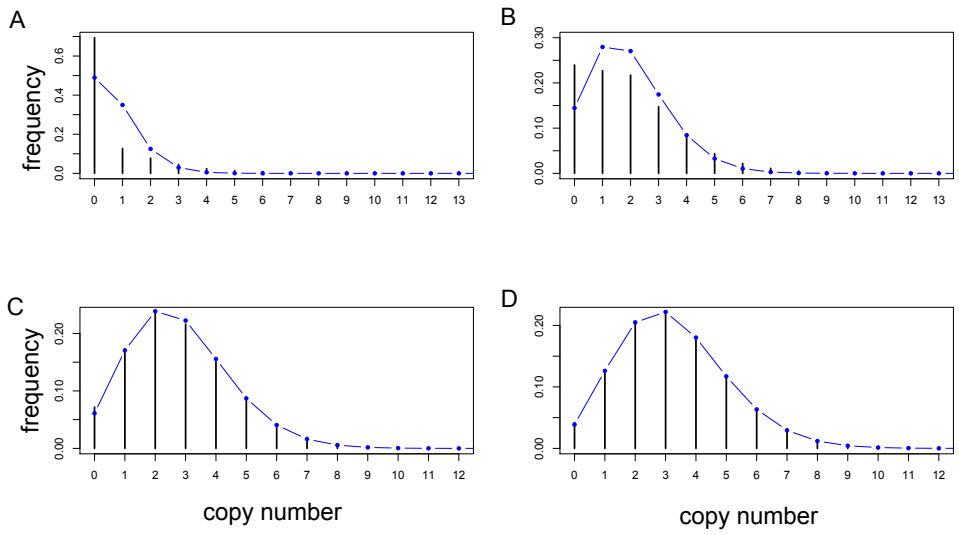

Figure S5 Distribution of TE copy number among host individuals at generation 15 (A), 25 (B), 35 (C) and 45 (D). Black bars are the simulated values while the blue dots are the *Poisson* expectation. The distribution of TE copy number reaches nearly *Poisson* around generation 35, when the *P cycotype* start being common in the population.

Our analytical model initially overestimates the host allele frequency. This is potentially caused by that fact that the *Poisson* approximation has a larger mode than the real copy number distribution. Because the copy number of an individual is generally small and the probability of hybrid dysgenic crosses happening is low, this did not lead to sever deviation between analytical predictions and the actual simulations.

After the *P element* in the population becomes common (around generation 35), our analytical model starts to predict lower host allele frequencies. This could be attributable to the transient linkage disequilibrium among TE insertions in the simulations. In this case, the simulation has a heavier right tail than the expectation from the *Poisson* approximation. The following tables (Table S5, 6, 7) show the proportion of simulations that have more individuals with a particular copy number than the predictions of the *Poisson* approximation. This proportion is universally greater than 50% for individuals with larger copy number, whose offspring are likely to have too many TE transpositions in a single generation. This can lead to stronger selection and a slightly higher host allele frequency change than the analytical model.

Table S5 The proportion of simulations that have more individuals with a particular copy number than the *Poisson* predictions at generation 40. This is the generation when the analytical model starts to underpredict the host allele frequency. The proportion of simulations that have more individuals with a particular copy number than the *Poisson* predictions are shown in the "Proportion" row, with proportion greater than 50% highlighted in blue. Individuals with large *P element* copy number may not present in all simulations and thus the "No Simulations" may not always be 1,000.

Copy Number	0	1	2	3	4	5	6	7	8	9	10	11	12	13	14	15	16	17	18
No Simulations	1000	1000	1000	1000	1000	1000	1000	1000	1000	1000	1000	1000	998	825	361	89	25	3	1
Proportion	1	0.017	0.06	0	0	0.034	0.968	1	1	1	1	0.992	0.92	0.976	1	1	1	1	1

Table S6 The proportion of simulations that have more individuals with a particular copy number than the *Poisson* predictions at generation 50.

Copy Number	0	1	2	3	4	5	6	7	8	9	10	11	12	13	14	15	16	17	18	19
No Simulations	1000	1000	1000	1000	1000	1000	1000	1000	1000	1000	1000	1000	1000	979	600	215	40	7	3	2
Proportion	1	0.011	0.701	0.493	0.134	0.072	0.271	0.833	0.985	0.979	0.906	0.811	0.692	0.618	1	1	1	1	1	1

Table S7 The proportion of simulations that have more individuals with a particular copy number than the *Poisson* predictions at generation 60.

Copy Number	0	1	2	3	4	5	6	7	8	9	10	11	12	13	14	15	16	17	18	22
No Simulations	1000	1000	1000	1000	1000	1000	1000	1000	1000	1000	1000	1000	1000	999	839	354	100	32	6	1
Proportion	0.969	0.001	0.661	0.854	0.646	0.3	0.233	0.362	0.605	0.652	0.618	0.537	0.517	0.48	0.613	1	1	1	1	1

Table S1 Sample locations of M strains

Continent	Country	specific position	name	stock number	Source
Africa	South Africa	Capetown	CA1	3846	BDSC[a]
	Zimbabwe	Kariba Dam	KSA2	3852	BDSC
		Kariba Dam	KSA3	3853	BDSC
		Kariba Dam	KSA4	3854	BDSC
Northern America	USA	South Carolina	Wild 10E	3892	BDSC
		North Carolina	Wild 11A	3893	BDSC
		North Carolina	Wild 11C	3894	BDSC
		North Carolina	Wild 11D	3895	BDSC
		New York	EV	3851	BDSC
		New York	MO1	3857	BDSC
		New York	Wild 1B	3880	BDSC
		Wisconsin	MWA1	3859	BDSC
		Wisconsin	Lausanne	4268	BDSC
		Ohio	Canton-S	1	BDSC
		Massachusetts	Amherst	4265	BDSC
		Illinoi	Urbana-S	4272	BDSC
		Oregon	Oregon-R	5	BDSC
		Riverside	RC1	3865	BDSC
		Riverside	RVC2	3869	BDSC
South America	Columbia	Bogata	BOG3	3843	BDSC
Asia	Japan	Iriomote island	IR98-01		M Itoh
		Iriomote island	IR98-06		M Itoh
		Hikone	HikoneR		M Itoh
	Russia	Uzbek Republic	Samarkand	4270	BDSC
Europe	Spain	Pyrenees	PYR3	3863	BDSC
	Portugal	Madeira	Reids1	3866	BDSC
	Greece	Athens	VAG2	3876	BDSC
		Athens	VAG3	3877	BDSC
	Sweden	Stockholm	Swedish-C	4271	BDSC

[a] Bloomington Drosophila Stock Center

Table S2 Linage-specific divergence on the *D. melanogaster* and *D. simulans* branches of TE-interacting and immunity genes

gene name	FBgn	*mel dN/dS*	*mel dN*	*mel dS*	*sim dN/dS*	*sim dN*	*sim dS*	functional class
Ago3	FBgn0250816	0.2614	0.0147	0.0563	0.2648	0.0208	0.0785	piRNA gene
armi	FBgn0041164	0.2973	0.0154	0.0518	0.3905	0.0222	0.0569	piRNA gene
aub	FBgn0000146	0.3824	0.0263	0.0687	0.5301	0.0338	0.0637	piRNA gene
krimp	FBgn0034098	0.4705	0.0342	0.0728	0.9641	0.0602	0.0625	piRNA gene
mael	FBgn0016034	0.9024	0.0324	0.0359	0.4907	0.0267	0.0545	piRNA gene
Hen1	FBgn0033686	0.2464	0.0159	0.0644	0.2658	0.0192	0.0721	piRNA gene
piwi	FBgn0004872	0.0807	0.0067	0.0836	0.1935	0.0093	0.0483	piRNA gene
rhi	FBgn0004400	1.4145	0.0764	0.054	0.5077	0.0556	0.1096	piRNA gene
Spn-E	FBgn0003483	0.2186	0.014	0.0642	0.2812	0.0166	0.0591	piRNA gene
squ	FBgn0002652	0.2399	0.0228	0.095	0.3376	0.0496	0.1469	piRNA gene
vas	FBgn0262526	0.2425	0.0453	0.1867	0.306	0.0437	0.143	piRNA gene
zuc	FBgn0261266	0.3585	0.0353	0.0985	0.2068	0.0214	0.1033	piRNA gene
Hrb27C	FBgn0004838	0.176	0.0021	0.0117	0.019	0.001	0.0538	P element gene
Irbp	FBgn0011774	0.1009	0.0088	0.0875	0.1635	0.0154	0.0944	P element gene
Ku80	FBgn0041627	0.1805	0.0125	0.069	0.245	0.0157	0.0642	P element gene
Psi	FBgn0014870	0.0908	0.0052	0.0575	0.0267	0.0011	0.0401	P element gene
AttA	FBgn0012042	0.0851	0.0151	0.178	0.1005	0.013	0.1294	effector
AttB	FBgn0041581	0.0351	0.0024	0.0677	0.0675	0.0062	0.0915	effector
AttC	FBgn0000276	0.0544	0.0085	0.1555	0.1263	0.0062	0.0489	effector
AttD	FBgn0038530	0.0948	0.0081	0.0851	0.3633	0.0158	0.0435	effector
Catsup	FBgn0002022	0.1012	0.009	0.0886	0.2507	0.0166	0.0662	effector
CecA1	FBgn0000276	0.0001	0	0.0648	NA	NA	NA	effector
CecA2	FBgn0000277	NA	NA	NA	NA	NA	NA	effector
CecB	FBgn0000278	0.0001	0	0.1231	0.3626	0.0069	0.0191	effector
CecC	FBgn0000279	0.0001	0	0.1431	NA	NA	NA	effector
CG11159	FBgn0034539	0.0001	0	0.0766	NA	NA	NA	effector
CG14823	FBgn0035734	0.1411	0.0102	0.072	0.188	0.0033	0.0176	effector
CG15293	FBgn0028526	0.4002	0.0353	0.0882	0.5249	0.0262	0.0499	effector
CG15825	FBgn0032773	0.1421	0.0152	0.1068	0.228	0.0072	0.0315	effector
CG16756	FBgn0029765	0.0854	0.0084	0.0985	0.1899	0.0173	0.0911	effector
CG16799	FBgn0034538	0.0678	0.0074	0.1092	0.1242	0.0047	0.0379	effector
CG18107	FBgn0034330	0.5364	0.0443	0.0825	0.0001	0	0.0543	effector
CG33470	FBgn0053470	NA	NA	NA	NA	NA	NA	effector
CG6421	FBgn0025827	0.1022	0.0101	0.0985	0.1508	0.0079	0.0523	effector
CG6426	FBgn0034162	0.062	0.0037	0.06	0.377	0.1255	0.3328	effector

CG6429	FBgn0046999	0.1226	0.0122	0.0999	0.0681	0.0099	0.1458	effector
CG6435	FBgn0034165	0.0001	0	0.0785	0.0581	0.0027	0.0469	effector
CG7798	FBgn0034092	0.0189	0.0029	0.1545	0.0001	0	0.0682	effector
CG8193	FBgn0033367	0.0235	0.0024	0.1001	0.0734	0.0089	0.1215	effector
CG8492	FBgn0035813	0.127	0.007	0.0552	0.1144	0.0069	0.0601	effector
Ddc	FBgn0000422	0.0184	0.0017	0.0904	0.0001	0	0.0413	effector
Def	FBgn0010385	0.1745	0.0151	0.0865	0.0001	0	0.0265	effector
Dpt	FBgn0004240	0.1002	0.011	0.1096	NA	NA	NA	effector
DptB	FBgn0034407	0.0811	0.0079	0.097	0.2091	0.0078	0.0373	effector
Dro	FBgn0010388	0.2487	0.0149	0.0601	0.3377	0.0144	0.0426	effector
Dro-2	FBgn0052279	0.0001	0	0.0665	0.1467	0.0124	0.0846	effector
Dro-3	FBgn0052283	NA	NA	NA	NA	NA	NA	effector
Dro-4	FBgn0052282	NA	NA	NA	0.0001	0	0.0186	effector
Dro-5	FBgn0035434	NA	NA	NA	0.0001	0	0.0263	effector
Dro6	FBgn0052268	0.2098	0.0123	0.0585	0.0676	0.006	0.0892	effector
Drs	FBgn0010381	NA	NA	NA	NA	NA	NA	effector
Drs-l	FBgn0052274	1.0897	0.0367	0.0337	0.0001	0	0.0615	effector
Duox	FBgn0031464	0.0028	0.0003	0.0986	0.0147	0.0011	0.0749	effector
Hml	FBgn0029167	0.0503	0.0046	0.0906	0.1561	0.0118	0.0757	effector
IM1	FBgn0034329	0.08	0.0108	0.1349	0.0001	0	0.041	effector
IM10	FBgn0033835	0.1533	0.0105	0.0686	0.2858	0.0222	0.0776	effector
IM2	FBgn0025583	0.0001	0	0.0917	0.2206	0.0109	0.0495	effector
IM23	FBgn0034328	NA	NA	NA	NA	NA	NA	effector
IM3	FBgn0040736	0.1634	0.0117	0.0717	0.0001	0	0.0339	effector
IM4	FBgn0040653	0.0001	0	0.0729	NA	NA	NA	effector
Irc	FBgn0038465	0.0771	0.0061	0.0796	0.0988	0.0069	0.0696	effector
Jafrac1	FBgn0040309	0.0001	0	0.1406	0.0001	0	0.0583	effector
Jafrac2	FBgn0040308	0.0001	0	0.0951	0.0001	0	0.0606	effector
LysB	FBgn0004425	NA	NA	NA	NA	NA	NA	effector
LysC	FBgn0004426	NA	NA	NA	NA	NA	NA	effector
LysD	FBgn0004427	NA	NA	NA	NA	NA	NA	effector
LysE	FBgn0004428	NA	NA	NA	NA	NA	NA	effector
LysP	FBgn0004429	NA	NA	NA	NA	NA	NA	effector
LysS	FBgn0004430	NA	NA	NA	NA	NA	NA	effector
LysX	FBgn0004431	0.273	0.0168	0.0614	0.1854	0.0122	0.066	effector
Mtk	FBgn0014865	0.0001	0	0.0246	0.178	0.0089	0.05	effector
ple	FBgn0005626	0.0357	0.0021	0.0598	0.0225	0.0007	0.0312	effector
Pu	FBgn0003162	0.097	0.004	0.0414	0.0001	0	0.0376	effector
Tig	FBgn0011722	0.0331	0.0043	0.1301	0.0573	0.0047	0.0822	effector

TotA	FBgn0028396	0.7779	0.0348	0.0447	0.6271	0.0222	0.0354	effector
TotB	FBgn0038838	0.435	0.0225	0.0517	0.5846	0.0278	0.0475	effector
TotC	FBgn0044812	NA	NA	NA	NA	NA	NA	effector
TotE	FBgn0053117	0.2167	0.0246	0.1137	0.1744	0.0087	0.0502	effector
TotF	FBgn0044811	NA	NA	NA	NA	NA	NA	effector
TotM	FBgn0031701	0.3909	0.0449	0.1148	0.2715	0.0193	0.0713	effector
TotX	FBgn0044810	0.3709	0.0247	0.0667	0.8708	0.0245	0.0282	effector
TotZ	FBgn0044809	0.0932	0.0033	0.0356	0.0001	0	0.0377	effector
Tsf1	FBgn0022355	0.0331	0.003	0.0915	0.0936	0.0113	0.1207	effector
Tsf2	FBgn0036299	0.0267	0.0021	0.0791	0.0272	0.002	0.0749	effector
Tsf3	FBgn0034094	0.0313	0.0029	0.0938	0.1219	0.007	0.0571	effector
yellow-f	FBgn0041710	0.1742	0.0137	0.0786	0.12	0.0141	0.1174	effector
yellow-f2	FBgn0038105	0.0778	0.0071	0.0907	0.1282	0.0078	0.061	effector
CG12780	FBgn0033301	0.1617	0.0159	0.0983	0.5244	0.0169	0.0323	recognition
CG13079	FBgn0032808	0.7221	0.0516	0.0715	0.4602	0.0294	0.0639	recognition
CG13422	FBgn0034511	0.1101	0.0176	0.1599	0.1177	0.0054	0.0456	recognition
CG30148	FBgn0050148	0.1991	0.0225	0.1131	0.463	0.0297	0.0642	recognition
CG31217	FBgn0051217	0.8493	0.0087	0.0103	0.1307	0.0068	0.0523	recognition
CG3212	FBgn0031547	0.459	0.0292	0.0636	0.463	0.0212	0.0458	recognition
CG6124	FBgn0243514	0.6973	0.048	0.0688	1.0046	0.0277	0.0276	recognition
Corin	FBgn0033192	0.0462	0.0035	0.0755	0.0799	0.0061	0.076	recognition
crq	FBgn0015924	0.1571	0.0088	0.0563	0.0875	0.0071	0.0812	recognition
emp	FBgn0010435	0.0001	0	0.0659	0.076	0.0032	0.0416	recognition
GNBP1	FBgn0040323	0.1069	0.0076	0.0706	0.0308	0.0018	0.0598	recognition
GNBP2	FBgn0040322	0.0698	0.0076	0.1086	0.1458	0.0057	0.039	recognition
GNBP3	FBgn0040321	0.0933	0.0064	0.0683	0.1986	0.0071	0.0356	recognition
He	FBgn0028430	1.0548	0.0873	0.0827	0.4288	0.0561	0.1307	recognition
Mcr	FBgn0020240	0.0186	0.0015	0.0826	0.0325	0.0015	0.0476	recognition
NimA	FBgn0261514	0.0459	0.0053	0.1156	0.0891	0.0064	0.072	recognition
NimB1	FBgn0027929	0.1212	0.0147	0.1209	0.2102	0.0112	0.0533	recognition
NimB2	FBgn0028543	0.0589	0.0051	0.0868	0.0232	0.002	0.084	recognition
NimB3	FBgn0054003	0.0799	0.0053	0.0663	0.3395	0.0163	0.048	recognition
NimB4	FBgn0028542	0.1125	0.0123	0.1092	0.1379	0.0168	0.1217	recognition
NimB5	FBgn0028936	0.1293	0.0068	0.0528	0.1955	0.0104	0.053	recognition
NimC1	FBgn0259896	0.5789	0.0335	0.0579	0.6331	0.0346	0.0547	recognition
NimC2	FBgn0028939	0.0964	0.0072	0.0746	0.1102	0.0052	0.0469	recognition
NimC3	FBgn0001967	0.1099	0.0098	0.0888	0.0001	0	0.0836	recognition
NimC4	FBgn0260011	0.0666	0.0081	0.1224	0.0627	0.0046	0.0732	recognition
pes	FBgn0031969	0.16	0.0085	0.0531	0.1808	0.0352	0.1947	recognition

PGRP-LA	FBgn0035975	0.1364	0.0113	0.0825	0.1091	0.0085	0.0778	recognition
PGRP-LB	FBgn0037906	0.1298	0.0073	0.056	0.051	0.0037	0.0731	recognition
PGRP-LC	FBgn0035976	0.1748	0.0122	0.07	0.1985	0.0119	0.0598	recognition
PGRP-LD	FBgn0260458	0.2447	0.01	0.0408	0.2587	0.0204	0.0787	recognition
PGRP-LE	FBgn0030695	0.0769	0.0052	0.0676	0.029	0.0025	0.0858	recognition
PGRP-LF	FBgn0035977	0.2456	0.0237	0.0966	0.2295	0.0157	0.0686	recognition
PGRP-SA	FBgn0030310	0.113	0.0106	0.0939	0.1491	0.0051	0.034	recognition
PGRP-SB1	FBgn0043578	0.03	0.0037	0.1248	0.274	0.0109	0.0397	recognition
PGRP-SB2	FBgn0043577	0.1484	0.0156	0.1051	0.0573	0.0022	0.0381	recognition
PGRP-SC1a	FBgn0043576	NA	NA	NA	NA	NA	NA	recognition
PGRP-SC1b	FBgn0033327	0.0001	0	0.1259	0.0314	0.002	0.0639	recognition
PGRP-SC2	FBgn0043575	0.0114	0.0022	0.1892	0.1564	0.0043	0.0277	recognition
PGRP-SD	FBgn0035806	0.1054	0.0076	0.072	0.3752	0.0073	0.0193	recognition
Sr-CI	FBgn0014033	0.3234	0.0428	0.1325	0.3326	0.0333	0.1003	recognition
Sr-CII	FBgn0020377	0.2926	0.0165	0.0562	0.1487	0.0087	0.0587	recognition
Sr-CIII	FBgn0020376	0.9783	0.0355	0.0363	0.3033	0.0136	0.0448	recognition
TepI	FBgn0041183	0.6271	0.0459	0.0732	0.7154	0.0324	0.0453	recognition
TepII	FBgn0041182	0.2017	0.0182	0.0902	0.2245	0.0169	0.0752	recognition
TepIII	FBgn0041181	0.0966	0.0053	0.0547	0.1046	0.0053	0.0507	recognition
TepIV	FBgn0041180	0.1581	0.0109	0.0692	0.2125	0.0081	0.0381	recognition
18w	FBgn0004364	0.0054	0.0004	0.0685	0.0241	0.0013	0.0521	signaling
Alk	FBgn0040505	0.0155	0.0013	0.0819	0.0148	0.0009	0.0599	signaling
aop	FBgn0000097	0.0332	0.0013	0.0383	0.1779	0.0045	0.0254	signaling
Atf-2	FBgn0050420	0.1091	0.0077	0.0703	0.1023	0.006	0.0588	signaling
ben	FBgn0000173	0.0001	0	0.0651	0.0001	0	0.0595	signaling
BG4	FBgn0038928	0.4744	0.0418	0.0881	0.7441	0.0358	0.0481	signaling
brm	FBgn0000212	0.007	0.0003	0.045	0.0204	0.0009	0.046	signaling
bsk	FBgn0000229	0.0001	0	0.033	0.0001	0	0.0187	signaling
cact	FBgn0000250	0.0418	0.0009	0.021	0.1454	0.0073	0.0502	signaling
caspar	FBgn0034068	0.0731	0.0057	0.0776	0.093	0.005	0.0539	signaling
CG11023	FBgn0031208	NA	NA	NA	NA	NA	NA	signaling
CG11501	FBgn0039666	0.2003	0.0253	0.1262	0.218	0.0431	0.1978	signaling
CG14225	FBgn0031055	NA	NA	NA	NA	NA	NA	signaling
CG16705	FBgn0039102	0.073	0.0087	0.1193	0.0924	0.0076	0.0826	signaling
CG2056	FBgn0030051	0.2411	0.0356	0.1477	NA	NA	NA	signaling
CG32382	FBgn0052382	0.2103	0.0224	0.1065	0.2277	0.0184	0.0808	signaling
CG32383	FBgn0052383	NA	NA	NA	NA	NA	NA	signaling
CG5896	FBgn0039494	0.0084	0.0014	0.1686	0.023	0.0014	0.0616	signaling
CG6361	FBgn0030925	0.2733	0.0246	0.0898	0.1544	0.0168	0.109	signaling

CG9675	FBgn0030774	0.2781	0.0205	0.0736	0.0827	0.0089	0.1077	signaling
cher	FBgn0014141	0.0029	0.0002	0.0636	0.0076	0.0004	0.0479	signaling
Dif	FBgn0011274	0.0742	0.0038	0.0517	0.3065	0.0195	0.0636	signaling
dl	FBgn0260632	0.0937	0.0055	0.0587	0.1534	0.0085	0.0553	signaling
Dnr1	FBgn0260866	0.0519	0.0051	0.0984	0.2411	0.0211	0.0877	signaling
dom	FBgn0020306	0.1153	0.0066	0.057	0.0918	0.0042	0.0458	signaling
dome	FBgn0043903	NA	NA	NA	NA	NA	NA	signaling
dpp	FBgn0000490	0.0244	0.0015	0.0628	0.1406	0.0041	0.0292	signaling
Dredd	FBgn0020381	0.2487	0.0217	0.0874	0.3217	0.018	0.0558	signaling
Dsor1	FBgn0010269	NA	NA	NA	NA	NA	NA	signaling
ea	FBgn0000533	0.0164	0.0011	0.065	0.0417	0.0032	0.0778	signaling
ECSIT	FBgn0028436	0.0694	0.0076	0.1099	0.0223	0.0021	0.0939	signaling
edl	FBgn0023214	0.1611	0.0158	0.0981	0.2673	0.013	0.0487	signaling
Egfr	FBgn0003731	0.0085	0.0009	0.1042	0.0723	0.005	0.0688	signaling
emb	FBgn0020497	0.0245	0.0008	0.0345	0.0001	0	0.0379	signaling
gcm	FBgn0014179	0.0567	0.0073	0.1279	0.1785	0.0072	0.0402	signaling
gcm2	FBgn0019809	0.0499	0.0035	0.0693	0.1858	0.019	0.1023	signaling
Hel89B	FBgn0022787	0.0745	0.0056	0.0748	0.0701	0.0032	0.0462	signaling
hep	FBgn0010303	0.1243	0.0069	0.0554	0.1565	0.0037	0.0234	signaling
hop	FBgn0004864	0.0244	0.0032	0.1333	0.1104	0.0043	0.0392	signaling
Iap2	FBgn0015247	0.0293	0.0013	0.0432	0.3387	0.0069	0.0205	signaling
imd	FBgn0013983	0.1094	0.0062	0.0566	0.0926	0.0031	0.0333	signaling
ird5	FBgn0024222	0.6424	0.0414	0.0644	0.5904	0.0264	0.0447	signaling
Jra	FBgn0001291	0.283	0.0128	0.0451	0.0218	0.0015	0.0712	signaling
kay	FBgn0001297	0.1724	0.0186	0.108	0.4523	0.0238	0.0527	signaling
key	FBgn0041205	0.6915	0.0358	0.0518	0.2065	0.0168	0.0815	signaling
kn	FBgn0001319	0.0001	0	0.0566	0.2697	0.0041	0.0153	signaling
lwr	FBgn0010602	0.0001	0	0.1845	0.0001	0	0.043	signaling
lz	FBgn0002576	0.0993	0.0054	0.0541	0.4277	0.0183	0.0427	signaling
mask	FBgn0043884	0.1113	0.0061	0.0544	0.1502	0.0064	0.0424	signaling
mbo	FBgn0026207	0.1619	0.0106	0.0656	0.3973	0.0218	0.055	signaling
Mekk1	FBgn0024329	0.1261	0.0068	0.0542	0.0374	0.0023	0.0618	signaling
Mkk4	FBgn0024326	0.0279	0.0021	0.0743	0.0001	0	0.0337	signaling
MP1	FBgn0027930	0.2143	0.0126	0.0589	0.3672	0.0184	0.0502	signaling
MP2	FBgn0037515	0.1428	0.0096	0.0671	0.2001	0.0105	0.0523	signaling
Mpk2	FBgn0015765	0.0508	0.0037	0.0722	0.0249	0.0012	0.0474	signaling
msn	FBgn0010909	0.02	0.0011	0.055	0.2116	0.0081	0.0381	signaling
MstProx	FBgn0015770	0.0001	0	0.0903	0.2794	0.0267	0.0954	signaling
mxc	FBgn0261524	0.0001	0	0.089	0.0001	0	0.0403	signaling

Myd88	FBgn0033402	0.0001	0	0.0579	0.0077	0.0008	0.1001	signaling
N	FBgn0004647	0.0348	0.0068	0.1949	0.0171	0.0016	0.0937	signaling
nec	FBgn0002930	0.1617	0.0161	0.0998	0.2151	0.0195	0.0907	signaling
Nos	FBgn0011676	0.0623	0.0042	0.0671	0.2299	0.018	0.0784	signaling
Ntf-2	FBgn0031145	0.0001	0	0.0304	0.0216	0.0033	0.1547	signaling
Ntf-2r	FBgn0032680	NA	NA	NA	NA	NA	NA	signaling
Nup214	FBgn0010660	0.2926	0.0159	0.0544	0.4797	0.0251	0.0522	signaling
os	FBgn0004956	0.0067	0.0007	0.1049	0.1633	0.0123	0.0756	signaling
p38b	FBgn0024846	0.0122	0.0012	0.0961	0.0001	0	0.0367	signaling
phl	FBgn0003079	0.042	0.0024	0.0567	0.0001	0	0.0313	signaling
pll	FBgn0010441	0.0083	0.001	0.1269	0.0693	0.0068	0.0977	signaling
pnt	FBgn0003118	0.0849	0.0071	0.0837	0.1334	0.0078	0.0583	signaling
POSH	FBgn0040294	0.0917	0.0039	0.0424	0.24	0.0081	0.0338	signaling
psh	FBgn0030926	0.0382	0.0058	0.1513	0.5135	0.0378	0.0736	signaling
puc	FBgn0243512	0.1645	0.0081	0.0494	0.2738	0.006	0.0218	signaling
Pvf1	FBgn0030964	0.017	0.0018	0.1039	0.0001	0	0.1067	signaling
Pvf2	FBgn0031888	0.1487	0.0141	0.0948	0.2669	0.0075	0.0281	signaling
Pvf3	FBgn0085407	0.0373	0.0056	0.15	0.0821	0.0022	0.0269	signaling
Pvr	FBgn0032006	0.0556	0.0051	0.0918	0.1103	0.0056	0.0505	signaling
Rac1	FBgn0010333	0.0001	0	0.054	0.0001	0	0.0509	signaling
Rac2	FBgn0014011	0.0001	0	0.0571	0.0001	0	0.0675	signaling
Ras85D	FBgn0003205	0.0001	0	0.0539	0.0001	0	0.0167	signaling
ref(2)P	FBgn0003231	0.5284	0.0209	0.0395	0.2144	0.0102	0.0475	signaling
Rel	FBgn0014018	0.4843	0.0287	0.0592	0.4329	0.0254	0.0586	signaling
RpS6	FBgn0261592	0.0232	0.0017	0.0729	0.0001	0	0.0418	signaling
SAE1	FBgn0029512	0.053	0.0054	0.102	0.0727	0.0052	0.0715	signaling
SAE2	FBgn0029113	0.1187	0.0053	0.0445	0.0989	0.0061	0.0618	signaling
Ser	FBgn0004197	0.1331	0.0046	0.0347	0.0692	0.0027	0.0386	signaling
slbo	FBgn0005638	0.0187	0.0038	0.2049	0.118	0.0115	0.097	signaling
slpr	FBgn0030018	0.0626	0.0055	0.0883	0.4856	0.0138	0.0284	signaling
smt3	FBgn0026170	0.0001	0	0.0561	0.0001	0	0.1209	signaling
Socs36E	FBgn0041184	0.1194	0.0084	0.0707	0.1435	0.0058	0.0405	signaling
Spn27A	FBgn0028990	0.0001	0	0.1094	0.1119	0.0056	0.0501	signaling
spz	FBgn0003495	0.199	0.0165	0.0827	0.2719	0.016	0.0589	signaling
srp	FBgn0003507	0.4695	0.0293	0.0624	0.3705	0.0194	0.0522	signaling
Stam	FBgn0027363	0.0571	0.0052	0.0905	0.2015	0.0122	0.0603	signaling
Stat92E	FBgn0016917	0.0263	0.0011	0.0433	0.1109	0.0057	0.0518	signaling
Su(H)	FBgn0004837	0.0001	0	0.0549	0.1309	0.0083	0.0634	signaling
Su(var)2-10	FBgn0003612	0.0804	0.0036	0.0449	0.0591	0.0008	0.0137	signaling

Tab2	FBgn0086358	0.1113	0.0076	0.0683	0.1541	0.005	0.0328	signaling
Tak1	FBgn0026323	0.1479	0.0082	0.0551	0.203	0.0066	0.0323	signaling
tamo	FBgn0041582	0.0761	0.0099	0.13	0.3117	0.0143	0.0457	signaling
Tehao	FBgn0026760	0.0413	0.0055	0.1321	0.1396	0.0081	0.0582	signaling
Thor	FBgn0261560	0.0437	0.0037	0.084	0.0001	0	0.0519	signaling
Tl	FBgn0262473	0.096	0.009	0.0935	0.0452	0.0037	0.0808	signaling
Toll-4	FBgn0032095	0.395	0.0219	0.0556	0.526	0.0236	0.0448	signaling
Toll-6	FBgn0036494	0.0191	0.0015	0.0773	0.0531	0.0021	0.0387	signaling
Toll-7	FBgn0034476	0.0118	0.0006	0.0538	0.0325	0.0013	0.0389	signaling
Toll-9	FBgn0036978	0.1592	0.0114	0.0717	0.1282	0.0083	0.0644	signaling
Tollo	FBgn0029114	0.0299	0.0017	0.0576	0.0468	0.0023	0.0501	signaling
Traf1	FBgn0026319	0.0001	0	0.1	0.0201	0.0009	0.0439	signaling
Traf2	FBgn0026318	0.0001	0	0.0548	0.0854	0.0068	0.079	signaling
Traf3	FBgn0030748	0.0523	0.0056	0.1075	0.0109	0.0009	0.0793	signaling
tub	FBgn0003882	0.2028	0.0084	0.0413	0.1457	0.0066	0.0451	signaling
Uev1A	FBgn0035601	0.0001	0	0.0239	NA	NA	NA	signaling
Ulp1	FBgn0027603	0.7093	0.0586	0.0827	0.9442	0.0671	0.0711	signaling
upd2	FBgn0030904	0.0333	0.0055	0.1655	0.2773	0.0032	0.0114	signaling
upd3	FBgn0053542	NA	NA	NA	NA	NA	NA	signaling
ush	FBgn0003963	0.1476	0.007	0.0473	0.5598	0.027	0.0482	signaling
WntD	FBgn0038134	0.0429	0.0029	0.0679	0.1115	0.0044	0.0392	signaling
ytr	FBgn0021895	0.2964	0.0024	0.0082	0.0001	0	0.0196	signaling

Table S3 Temporal and geographic differentiation of all candidate genes

	no. M strain	M strain π		*temporal differentiation*		*geographic differentiation*[b]	
		nonsyn	syn	*Fst*	*p-value*	*Fst*	*p-value*
AGO3	8	0.0000	0.0010	-0.067	0.824	0.125	0.121
armi	8	0.0015	0.0094	-0.045	0.897	0.237	**< 0.001**
aub	8	0.0009	0.0065	-0.045	0.883	0.484	**< 0.001**
Hen1	30	0.0013	0.0097	**0.303**	**0.001**	0.632	**< 0.001**
Hrb27C	8	0.0008	0.0025	0.048	0.153	0.116	0.083
Irbp	30	0.0020	0.0058	**0.170**	**0.038**	0.144	0.111
krimp	30	0.0076	0.0304	0.011	0.262	0.143	**0.004**
Ku80	8	0.0018	0.0134	-0.035	0.891	0.256	**0.001**
mael	8	0.0015	0.0000	-0.061	0.98	0.344	**< 0.001**
piwi	8	0.0011	0.0121	0.051	0.092	0.172	**0.006**
Psi	8	0.0007	0.0123	0.034	0.204	0.338	**< 0.001**
rhi	8	0.0017	0.0056	-0.013	0.469	0.236	**0.013**
Spn-E	30	0.0010	0.0033	0.053	0.08	0.459	**< 0.001**
squ	30	0.0016	0.0080	**0.202**	**0.001**	0.028	0.25
vas	8	0.0005	0.0045	0.025	0.223	0.213	**0.003**
zuc	8	0.0000	0.0054	-0.052	0.797	0.284	**0.005**

[a]Genetic differentiation between current (*post-P element*) African and North American populations
[b]Genetic differentiation between *pre-P* and *post-P* element invasion populations
All the significant results are in bold-type

Table S4 Information of Control Genes

symbol	FBgn	gene functions
jeb	FBgn0086677	visceral mesoderm development
CG8378	FBgn0027495	negative regulation of transcription
CG13178	FBgn0033685	cilium assembly
CG8878	FBgn0027504	protein serine/threonine kinase; protein phosphorylation
CG8407	FBgn0033687	microtubule-based movement
Oda	FBgn0014184	cell differentiation; embryonic development
wash	FBgn0033692	GTPase binding; signal transductions; actin filament and microtubule bundles assembly
CG33964	FBgn0053964	unknown
Cyp6t3	FBgn0033697	oxidation-reduction process
RpS11	FBgn0033699	structural constituent of ribosome; translation; mitotic spindle organization
Sr-CII	FBgn0020377	scavenger receptor activity; defense response